COA 2016 中国海洋声学研讨会
IEEE/OES China Ocean Acoustics Symposium
Harbin, China | January 9-11, 2016

Underwater Acoustic Scattering of Bessel Beam by Spherical Shell Using T-matrix Method*

LIU Shuigen
Naval military representative office in China ship development and design center
Wuhan, P.R. China

GONG Zhixiong, CHAI Yingbin
School of naval architecture and ocean engineering
Huazhong university of science and technology
Wuhan, P.R. China
hustgzx@hust.edu.cn

LI Wei
School of Naval Architecture and Ocean Engineering
Huazhong University of Science and Technology
Wuhan, P.R. China
Collaborative Innovation Center for Advanced Ship and Deep-Sea Exploration (CISSE)
Shanghai, P.R. China

***Abstract*—The Bessel beam has been proved to show several advantages over the plane wave for its superior characteristics, including nondiffraction and self-reconstruction properties. The Bessel beam is characterized by an important parameter, called the half-conical angle, which describes the angle of the planar wave components of the beam relative to the beam axis. In this research paper, the T-matrix method (TMM) is combined with a Bessel beam to compute the acoustic scattering field. The backscattering form functions of a tungsten carbide sphere and a steel spherical shell are calculated and curved as a function of dimensionless frequency. Several Rayleigh resonance patterns are depicted to further confirm the orders of resonance. By selecting appropriate half-conical angles, several corresponding resonances can be suppressed and this phenomenon may have some potential value in practical applications.**

***Keywords*—T-matrix method; Bessel beam; acoustic scattering; form function; spherical shell**

I. INTRODUCTION

In the past few decades, there has been considerable interest by many researchers in the study of acoustic resonance scattering by underwater elastic targets in plane waves, through experimental and theoretical methods [1-6]. Generally, resonance scattering fields will carry some useful information relevant to unknown scatterers and this will help to develop new techniques for the detection, location and recognition of underwater objects. To identify the resonance mode orders of an elastic object, the pure resonance scattering amplitude (RSA) should be obtained first. To this end, Flax, Dragonette and Überall first utilized theoretical methods by subtracting a specularly reflected wave amplitude from the total scattering amplitude (TSA) [1]. For the same purpose, experimental methods have also been devised, including the MIIR method [7-8] and the method of Billy [9]. In the present paper, the T-matrix method, which belongs to the theoretical separation method, is adopted to calculate the pure RSA and has been demonstrated to be effective for an elastic sphere [10].

Recently, the Bessel beam has been developed rapidly in optics [11-12], electromagnetics [13-14] and acoustics [15-17]. It is demonstrated that the Bessel beam has several advantages over ordinary plane waves with the characteristics of non-diffraction [18] and the ability to self-reconstruct[19]. To our knowledge, exploration of a method of using the characteristics of acoustic Bessel beams is somewhat limited. In the literatures published [20], [16], partial wave series expansion (PWSE) is the main method of studying acoustic Bessel scattering. Hence, we combine the TMM with the Bessel beam to overcome the shortcomings of PWSE and introduce a powerful tool for further exploration on acoustic scattering under the illumination of a Bessel beam.

II. THEORETICAL FORMULATION

A. T-matrix method

In this section, we briefly give the theoretical formulas of an elastic scatterer immersed in fluid interacted with an ideal acoustic Bessel beam by using TMM. To obtain the transition matrix, the integral representations for the displacement fields, the boundary conditions and expansions of surface fields should be provided first.

Now consider an elastic scatterer with its geometry shown in Fig. 1, the host medium is homogeneous water with density ρ, Lame parameter λ and wavenumber k. The layered object has an empty core (a cavity) surrounded by an elastic layer with density ρ_0, Lamb parameters λ_0 and μ_0, and longitudinal and transverse wavenumbers k_p and k_s, respectively. The time factor $e^{-i\omega t}$ is suppressed throughout. The outer surface of the object is denoted by S and inner by S_0,

Work supported by the National Natural Science Foundation of China under Grant No. 51579112.

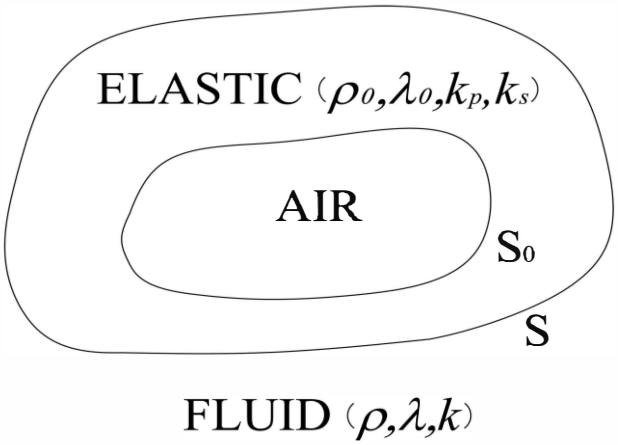

Fig. 1. Geometry of a layered obstacle

and their unit normal $\hat{n}$ and $\hat{n}_0$ are taken as outward pointing. The explanations of the following variables are given in detail in [21].

The integral representations for the displacement fields in the fluid and in the elastic layer are given as follows:

$$\mathbf{u}^i + k\int_S [\hat{n}\cdot\mathbf{u}_+(\nabla\cdot\mathbf{G}) - \nabla\cdot\mathbf{u}_+\hat{n}\cdot\mathbf{G}]\mathrm{d}S = \begin{cases}\mathbf{u} & \mathbf{r} \text{ outside } S\\ 0 & \mathbf{r} \text{ inside } S\end{cases} \tag{1}$$

$$-\frac{k_s}{\mu_0}\int_S [\mathbf{u}_-\cdot(\hat{n}\cdot\boldsymbol{\Sigma}_0) - \mathbf{t}_-\cdot\mathbf{G}_0]\mathrm{d}S + \frac{k_s}{\mu_0}\int_{S_0}[\mathbf{u}_+\cdot(\hat{n}_0\cdot\boldsymbol{\Sigma}_0) - \mathbf{t}_+^0\cdot\mathbf{G}_0]\mathrm{d}S$$
$$= \begin{cases}\mathbf{u} & \mathbf{r} \text{ between } S \text{ and } S_0\\ 0 & \mathbf{r} \text{ outside } S \text{ or inside } S_0\end{cases} \tag{2}$$

Green's dyadic in fluid and elastic layer are expanded in spherical harmonic functions respectively:

$$\mathbf{G}(\mathbf{r},\mathbf{r}') = i\sum \mathrm{Re}\Phi_n(\mathbf{r}_<)\Phi_n(\mathbf{r}_>) \tag{3}$$

$$\mathbf{G}_0(\mathbf{r},\mathbf{r}') = i\sum \mathrm{Re}\psi_{\tau n}(\mathbf{r}_<)\psi_{\tau n}(\mathbf{r}_>) \tag{4}$$

And the incoming and scattering fields

$$\mathbf{u}^i = \sum a_n \mathrm{Re}\Phi_n \tag{5}$$

$$\mathbf{u}^S = \sum f_n\Phi_n, \quad r > \max_{r'\in S} r' \tag{6}$$

Substitute (3)-(6) into (1) and (2), the integral representations of incident and scattered coefficients can be derived immediately.

$$a_n = -ik\int_S [\hat{n}\cdot\mathbf{u}_+\nabla\cdot\Phi_n - \nabla\cdot\mathbf{u}_+\hat{n}\cdot\Phi_n]\mathrm{d}S \tag{7}$$

$$f_n = ik\int_S [\hat{n}\cdot\mathbf{u}_+\nabla\cdot\mathrm{Re}\Phi_n - \nabla\cdot\mathbf{u}_+\hat{n}\cdot\mathrm{Re}\Phi_n]\mathrm{d}S \tag{8}$$

The corresponding boundary conditions on outer surface S and inner surface S_0 are listed in the following expressions:

$$\begin{cases}\left.\begin{aligned}&\hat{n}\cdot\mathbf{u}_+ = \hat{n}\cdot\mathbf{u}_-;\\ &\lambda\nabla\cdot\mathbf{u}_+ = \hat{n}\cdot\mathbf{t}_-;\\ &\hat{n}\times\mathbf{t} = 0\end{aligned}\right\} & \text{on } S\\ \left.\mathbf{t}_+^0 = 0\right\} & \text{on } S_0\end{cases} \tag{9}$$

Finally, the incident and total scattered field coefficients are related through the transition as given by

$$f_n = \sum_{n'} T_{n,n'}a_{n'} \tag{10}$$

And the transition matrix

$$f_n = \sum_{n'} T_{n,n'}a_{n'} \tag{11}$$

$$\begin{aligned}\mathbf{T} = &-[\mathrm{Re}\mathbf{Q}(\mathrm{Re}\mathbf{R}+\mathbf{T}^0\mathbf{P})^{-1}(\mathrm{Re}\mathbf{P}+\mathbf{T}^0\mathbf{P}) - \mathrm{Re}\mathbf{M}]\\ &\times[\mathbf{Q}(\mathrm{Re}\mathbf{R}+\mathbf{T}^0\mathbf{R})^{-1}(\mathrm{Re}\mathbf{P}+\mathbf{T}^0\mathbf{P}) - \mathbf{M}]^{-1}\end{aligned} \tag{12}$$

where

$$\mathbf{T}^0 = -\mathrm{Re}\mathbf{Q}^0(\mathbf{Q}^0)^{-1} \tag{13}$$

Specially, when $\mathbf{T}_0 = 0$, (11) yields the transition matrix for a homogeneous elastic body in water. To acquire the pure scattering field, a rigid background should be subtracted from the total scattered coefficients in (10),

$$f_n^{pure} = \sum_{n'}\left(T_{n,n'} - T_{n,n'}^{\mathrm{rigid}}\right)a_{n'} \tag{14}$$

The details of $T_{n,n'}^{\mathrm{rigid}}$ can be found in [17].

B. Incident coefficients of the Bessel beam

In the case of Bessel beam incidence, the incident coefficients of expression are obviously different from those of an ordinary plane wave. By using the spherical harmonic expansion and addition theorem of the Legendre polynomial,

978-1-4673-9978-4/16/$31.00 ©2016 IEEE

the incident coefficients under an ideal zeroth-order Bessel beam are as follows

$$a_{nm\sigma} = 4\pi\xi_{nm} i^n \times P_n^m(\cos\theta_i) P_n^m(\cos\beta) \begin{pmatrix} \cos(m\varphi), & \sigma = \mathrm{e} \\ \sin(m\varphi), & \sigma = \mathrm{o} \end{pmatrix} \quad (15)$$

III. NUMERICAL EXAMPLES

In order to study the Bessel beam's modification to the coupling to resonances of elastic scatterers, two numerical examples are presented by using the T-matrix method, including an elastic sphere and spherical shell.

A. Sphere

In the first part, the tungsten carbide (WC) sphere will be discussed. The backscattering form functions are used to describe the far-fields characteristics of the WC sphere immersed in water under the illumination of the ideal zeroth-order Bessel beam. The longitudinal and shear velocities of the elastic sphere are 6650 m/s and 3981m/s, respectively. The density of WC is 13.8 g/cm^3. The fluid considered here is water with velocity $c = 1482.5$ m/s and $\rho = 1$ g/cm^3.

To facilitate the discussion in the following, several half-conical angles are selected specially which are defined β_n as the lowest root of $P_n(\cos\beta_n) = 0$. The 6-digit approximations to β_n for $n = 2,3,4$ and 5 are $\beta_2 = 54.7346^\circ$, $\beta_3 = 39.2315^\circ$, $\beta_4 = 30.5556^\circ$ and $\beta_5 = 25.0173^\circ$, respectively.

Figs. 2-4 plot rigid, total and pure backscattering form function modulus versus dimensionless frequency ka for a WC sphere in water illuminated by a Bessel beam with the different selective half-conical angles given above. $\beta = 0$ gives the case of plane wave illumination. It is shown that after subtracting the rigid backscattering from the total, the pure backscattering can be obtain immediately. By selecting the lowest roots of $P_n(\cos\beta_n) = 0$, the corresponding nth order Rayleigh resonance is suppressed. The first five orders of Rayleigh resonance can be clearly identified at $ka = 1.45$, 7.06, 10.46, 13.38 and 16.10. The corresponding bistatic patterns of Rayleigh resonance are depicted in Figs. 5-9. This demonstrates the accuracy of resonance orders by the lobe numbers in bistatic patterns and the suppression effect of selective Bessel beams.

B. Spherical shell

In the second part, the steel spherical shell will be discussed. Similarly, the backscattering form functions are also studied. The longitudinal and shear velocities of steel are 5854 m/s and 3150m/s, respectively. The density of WC is 7.84 g/cm3. The fluid considered here is also water. The rigid, total and pure backscattering form function modulus versus dimensionless frequency ka for a steel spherical shell in water illuminated by

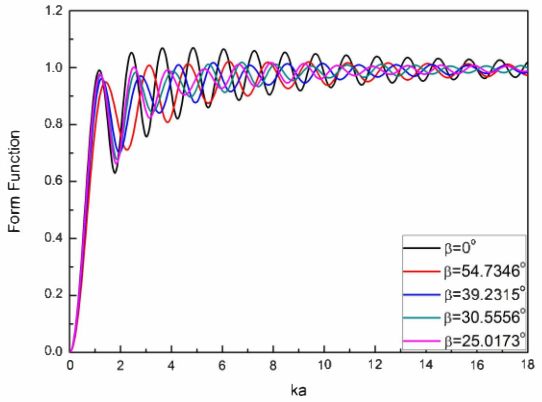

Fig. 2. Rigid backscattering form function modulus versus dimensionless frequency ka for a WC sphere in water illuminated by Bessel beam

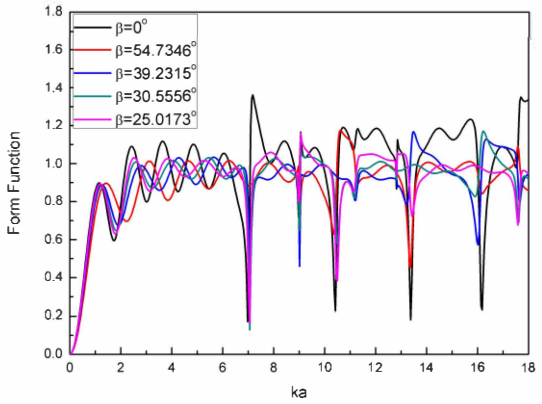

Fig. 3. Total backscattering form function modulus versus dimensionless frequency ka for a WC sphere in water illuminated by Bessel beam

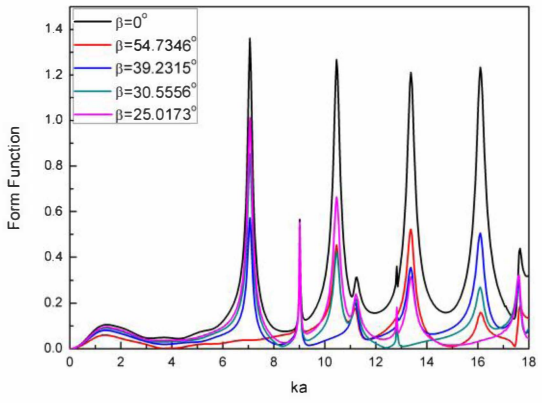

Fig. 4. Pure backscattering form function modulus versus dimensionless frequency ka for a WC sphere in water illuminated by Bessel beam

978-1-4673-9978-4/16/$31.00 ©2016 IEEE

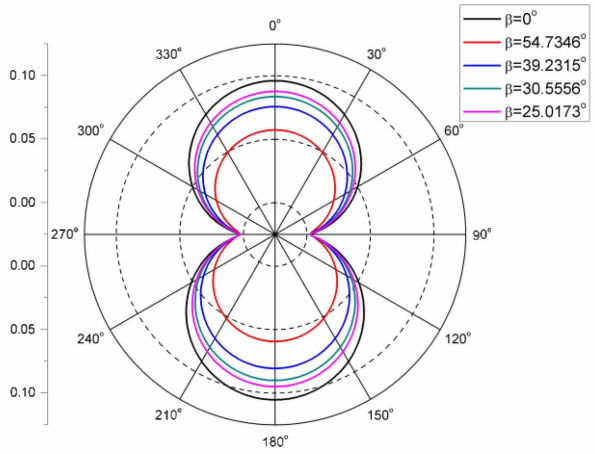

Fig. 5. Bistatic pattern of first-order Rayleigh resonance of a WC sphere in water when $ka = 1.45$

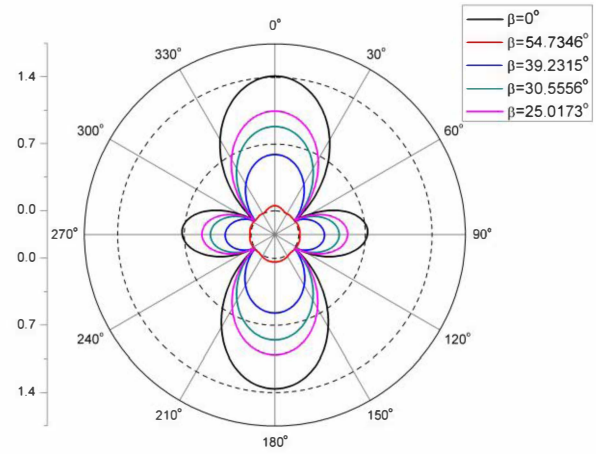

Fig. 6. Bistatic pattern of second-order Rayleigh resonance of a WC sphere in water when $ka = 7.06$

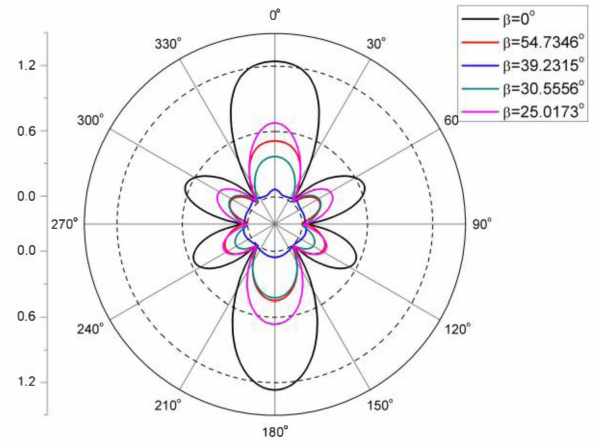

Fig. 7. Bistatic pattern of third-order Rayleigh resonance of a WC sphere in water when $ka = 10.46$

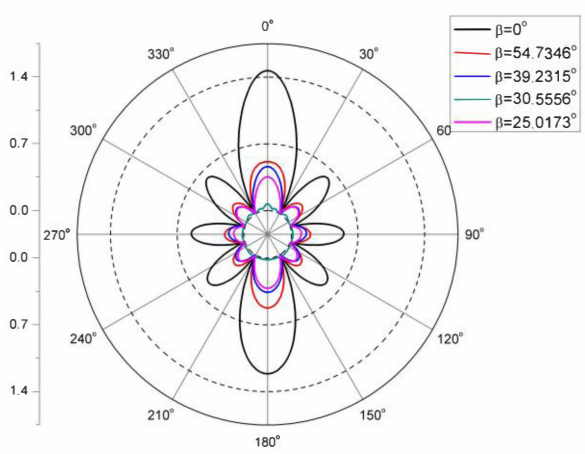

Fig. 8. Bistatic pattern of fourth-order Rayleigh resonance of a WC sphere in water when $ka = 13.38$

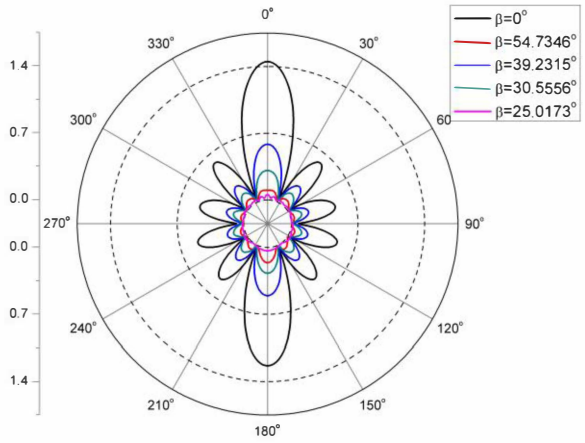

Fig. 9. Bistatic pattern of fifth-order Rayleigh resonance of a WC sphere in water when $ka = 16.10$

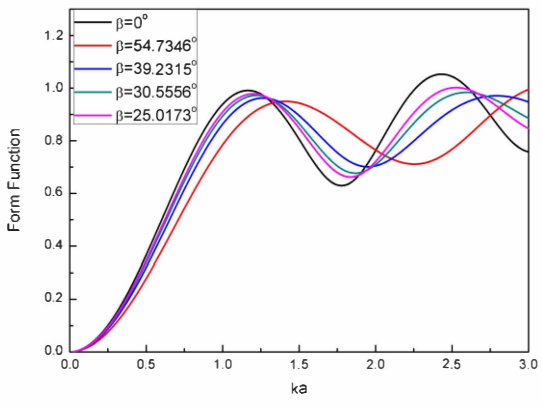

Fig. 10. Rigid backscattering form function modulus versus dimensionless frequency ka for a steel spherical shell in water illuminated by Bessel beam

978-1-4673-9978-4/16/$31.00 ©2016 IEEE

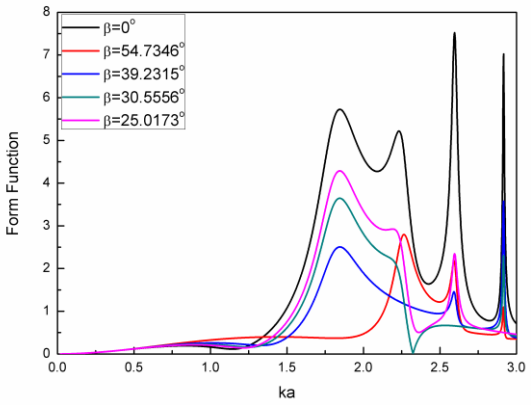

Fig. 11. Total backscattering form function modulus versus dimensionless frequency ka for an steel spherical shell in water illuminated by Bessel beam

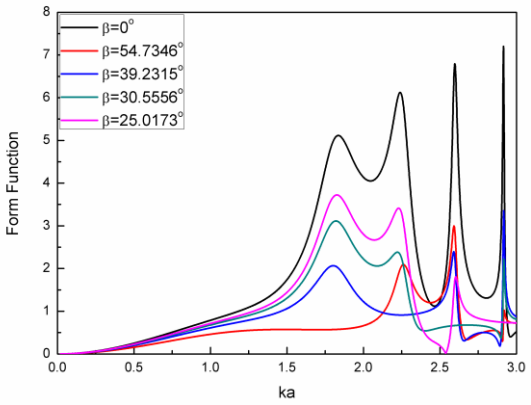

Fig. 12. Pure backscattering form function modulus versus dimensionless frequency ka for an steel spherical shell in water illuminated by Bessel beam

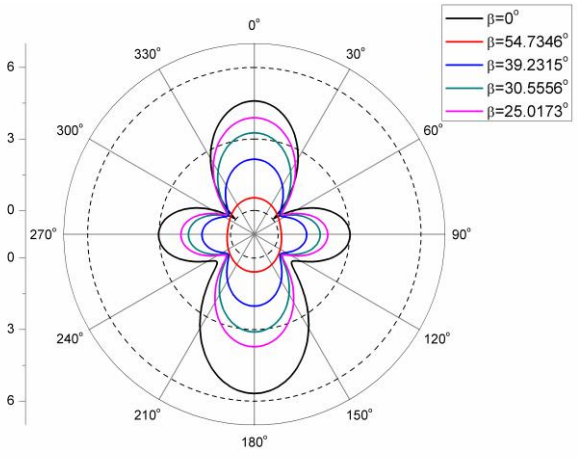

Fig. 13. Bistatic pattern of second-order Rayleigh resonance of a steel spherical shell in water when $ka = 1.836$

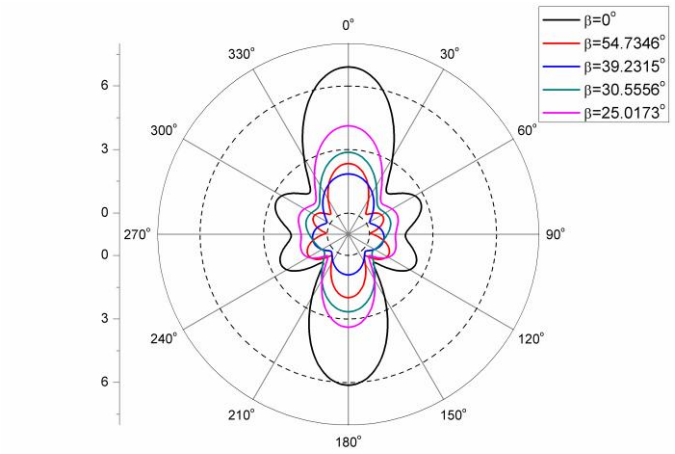

Fig. 14. Bistatic pattern of third-order Rayleigh resonance of a steel spherical shell in water when $ka = 2.24$

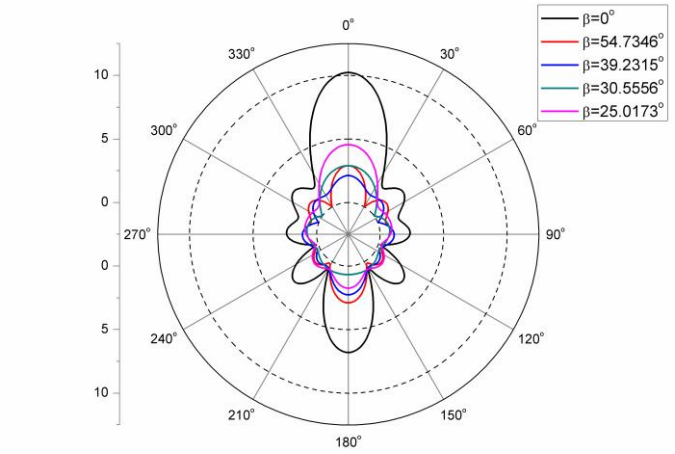

Fig. 15. Bistatic pattern of fourth-order Rayleigh resonance of a steel spherical shell in water when $ka = 2.597$

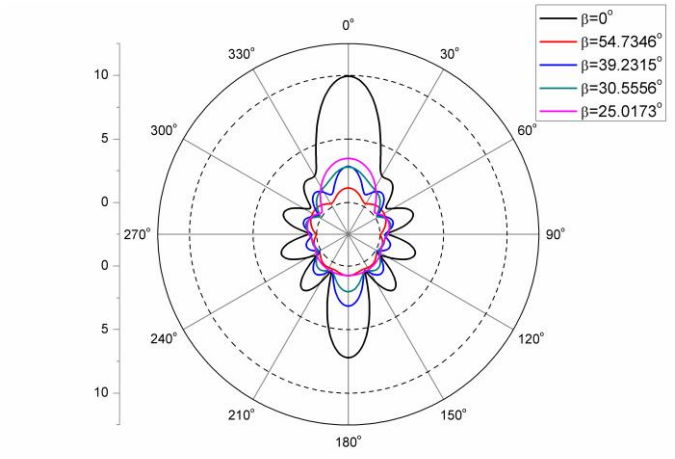

Fig. 16. Bistatic pattern of fifth-order Rayleigh resonance of a steel spherical shell in water when $ka = 2.915$

978-1-4673-9978-4/16/$31.00 ©2016 IEEE

a Bessel beam with different selective half-conical angles are plotted in Figs. 10-12, respectively. The bistatic patterns of Rayleigh resonance are also drawn in Figs. 13-16. The conclusion is the same as for a sphere.

IV. CONCLUSIONS

In this paper, two numerical examples are carried out to calculate the backscattering form functions of an underwater WC sphere and a steel spherical shell illuminated by a zeroth-order Bessel beam with several selective half-conical angles. The T-matrix method is implemented and is demonstrated to be an effective tool to compute the scattered fields. The orders of Rayleigh resonance can be identified by the lobe number in bistatic patterns. With appropriate selection of specific Bessel beam parameters, some resonances can be suppressed and this, in turn, may provide useful directions for engineering applications. Moreover, the T-matrix method is able to expand its range of applicability to study complex objects when interacted with a Bessel beam by improving its integration procedure; this is our interest for future work.

REFERENCES

[1] L. Flax, L.R. Dragonette, and H. Überall, "Theory of elastic resonance excitation by sound scattering," J. Acoust. Soc. Am., Vol. 63, pp. 723-731, 1978.

[2] G.C.Gaunaurd and H. Überall, "RST analysis of monostatic and bistatic acoustic echoes from an elastic sphere," J. Acoust. Soc. Am., Vol. 73, pp. 1-12, 1983.

[3] M.F. Werby, H. Überall, A. Nagl, S.H. Brown, and J.W. Dickey, "Bistatic scattering and identification of the resonances of elastic spheroids," J. Acoust. Soc. Am., Vol. 84, pp. 1425-1436, 1988.

[4] K.L. Williams and P.L. Marston, "Synthesis of backscattering from an elastic sphere using the Sommerfeld–Watson transformation and giving a Fabry–Perot analysis of resonances," J. Acoust. Soc. Am., Vol. 79, pp. 1702-1708, 1986.

[5] X.L. Bao, H. Überall, and Jan Niemiec, "Experimental study of sound scattering by elastic spheroids, and the excitation of their resonances," J. Acoust. Soc. Am., Vol. 92, pp. 2313-2314, 1992.

[6] L. Haumesser, D. Décultot, F. Léon, and G. Maze, "Experimental identification of finite cylindrical shell vibration modes," J. Acoust. Soc. Am., Vol. 111, PP. 2034-2039, 2002.

[7] G. Maze and J. Ripoche, "Visualization of acoustic scattering by elastic cylinders at low ka," J. Acoust. Soc. Am., Vol. 73, pp. 41-43, 1983.

[8] G. Maze, J.L. Izbicki, and J. Ripoche, "Resonances of plates and cylinders: Guided waves," J. Acoust. Soc. Am., Vol. 77, pp. 1352-1357, 1985.

[9] M. De Billy, "Determination of the resonance spectrum of elastic bodies via the use of short pulses and Fourier transform theory," J. Acoust. Soc. Am., Vol. 79, pp. 219-221, 1986.

[10] M.W. Werby and H. Überall, "Bistatic cross sections and the resonance order: The Rayleigh wave dipole resonance," J. Acoust. Soc. Am., Vol. 82, pp. 265-269, 1987.

[11] Z. Bouchal, J. Wagner, and M. Chlup, "Self-reconstruction of a distorted nondiffracting beam," Opt. Commun., Vol. 151, pp. 207-211, 1998.

[12] Z. Chen, Y. Han, Z Cui, and X. Shi, "Scattering analysis of Bessel beam by a multilayered sphere," Opt. Commun., Vol. 340, pp. 5-10, 2015.

[13] F.G. Mitri, "Arbitrary scattering of an electromagnetic zero-order Bessel beam by a dielectric sphere," Opt. Lett., Vol. 36, pp. 766-768, 2011.

[14] F.G. Mitri, R.X. Li, L.X. Guo, and C.Y. Ding, "Resonance scattering of a dielectric sphere illuminated by electromagnetic Bessel non-diffracting (vortex) beams with arbitrary incidence and selective polarizations," Ann. Phys., Vol. 361, pp. 120-147, 2015.

[15] P.L. Marston, "Axial radiation force of a Bessel beam on a sphere and direction reversal of the force," J. Acoust. Soc. Am., Vol. 120, pp. 3518-3524, 2006.

[16] F.G. Mitri, "Acoustic scattering of a high-order Bessel beam by an elastic sphere," Ann. Phys., Vol. 323, pp. 2840-2850, 2008.

[17] W. Li, J. Li, and Z.X. Gong, "Study on underwater acoustic scattering of a Bessel beam by rigid objects with arbitrary shapes," Acta Phys. Sin., Vol. 64, 154305, 2015.

[18] J. Durnin, J.J. Miceli Jr, and J.H. Eberly, "Diffraction-free beams," Phys. Rev. Lett., Vol. 58, pp. 1499-1501, 1987.

[19] Z. Bouchal, J. Wagner, and M. Chlup, "Self-reconstruction of a distorted nondiffracting beam," Opt. Commun., Vol. 151, pp. 207-211, 1998.

[20] P.L. Marston, "Scattering of a Bessel beam by a sphere," J. Acoust. Soc. Am., Vol. 121, pp. 753-758, 2007.

[21] W. Li, Ph.D. Dissertation, Singapore: National University of Singapore, 2004.

978-1-4673-9978-4/16/$31.00 ©2016 IEEE